Three-dimensional alignment of cellulose II microcrystals under a strong magnetic field

Masahisa Wada (ID) · **Sayuri Wakiya · Kayoko Kobayashi · Satoshi Kimura ·**
Motomitsu Kitaoka · Ryosuke Kusumi · Fumiko Kimura · Tsunehisa Kimura

Abstract In this study, enzymatic synthesis was conducted using cellodextrin phosphorylase (CDP), sucrose phosphorylase (SP), and sucrose with 1-azido-1-deoxy-β-glucoside (β-glucosyl azide) as the acceptor in phosphate buffer at pH 7.0. This yielded cellulose oligomers (degree of polymerization, DP ≈ 10) with azido groups at the reducing end as a white precipitate. A suspension of cellulose microcrystals with exposed azido groups on the surface was obtained via dissolution and recrystallization of the synthetic products dispersed in water by heating. The flat, ribbon-like cellulose microcrystals were a crystalline form of cellulose II and were several micrometers in length and several hundred nanometers in width. The microcrystals were 5.1–5.2 nm thick, which is equivalent to the chain length of cellulose oligomers with DP ≈ 10. When the cellulose II microcrystal suspensions were dried under a horizontal static magnetic field of 8 T, oriented films were obtained, wherein the microcrystals were aligned three-dimensionally. Synchrotron X-ray diffraction studies of the films revealed that the easy and intermediate axes (χ_1 and χ_2, respectively) of the cellulose II crystals corresponded approximately to the [1 1 0] and [1 $\overline{1}$ 0] directions, respectively.

Keywords Cellulose II · Cellulose oligomer crystal · Transmission electron microscopy · Magnetic field · Synchrotron X-ray diffraction

M. Wada (✉) · S. Wakiya · K. Kobayashi ·
R. Kusumi · F. Kimura · T. Kimura
Graduate School of Agriculture, Kyoto University,
Kyoto 606-8502, Japan
e-mail: wada.masahisa.8c@kyoto-u.ac.jp

M. Wada · S. Kimura
College of Life Science, Kyung Hee University,
Yongin-si 446-701, Gyeonggi-do, Korea

S. Kimura
Graduate School of Agricultural and Life Sciences, The
University of Tokyo, Tokyo 113-8657, Japan

M. Kitaoka
Faculty of Agriculture, Niigata University, 8050 Ikarashi
2-no-cho, Nishi-ku, Niigata 950-2181, Japan

T. Kimura
Fukui University of Technology, 3-6-1 Gakuen,
Fukui 910-8505, Japan

Introduction

Cellulose is the most abundant organic polymer on Earth and is a promising raw material in terms of renewability and sustainability for the preparation of various functional materials. In nature, cellulose molecular chains are biosynthesized, bundled, and crystallized, existing as slender nanosized rods and microfibrils (Preston and Ripley 1954). Cellulose nanocrystals (CNCs) can be prepared via the acid

hydrolysis of natural cellulose: cellulose I (Rånby 1949, 1951; Rånby and Ribi 1950; Marchessault et al. 1959). The dimension of CNCs range from 3 to 20 nm in width and more than 1 μm in length depending on their origin (Habibi et al. 2008; Klemm et al. 2011).

Achieving the optimal orientation of CNCs is an important technique for improving the physical and mechanical properties of nanocomposites. Several attempts have been made to align CNCs using shearing force (Nishiyama et al. 1997), electric fields (Bordel et al. 2006; Habibi et al. 2008), and magnetic fields (Sugiyama et al. 1992; Revol et al. 1994; Dong and Gray 1997; Pullawan et al. 2012). Among these, the magnetic field is characterized by its penetration of the CNCs. It has been reported that the easy axis (χ_1) of the CNC is approximately perpendicular to the glucose rings, and the hard magnetization axis (χ_3) is parallel to the chain axis (the *c*-axis) (Nilakantan 1938; Frka-Petesic et al. 2015). Under a static magnetic field, the χ_1 axis aligns parallel to the magnetic field. The uniaxial orientation of the χ_3 axis (parallel to the *c*-axis) is achieved by a rotating magnetic field (Kimura et al. 2005; Song et al. 2013), and the three-dimensional orientation is achievable using a modulated rotating magnetic field (Kimura and Kimura 2009). However, no studies have been reported on the magnetic orientation of cellulose II, another important polymorph of cellulose.

Cellulose II is generally prepared via the dissolution/regeneration or mercerization of native cellulose. The crystal structure of cellulose II has been revealed using a combination of synchrotron X-ray and neutron diffraction (Langan et al. 1999, 2001). Cellulose II adopts a two-chain monoclinic unit cell (space group $P2_1$, $a = 8.10$ Å, $b = 9.03$ Å, $c = 10.31$ Å, and $\gamma = 117.1°$), where the chains with opposite polarities are packed in an antiparallel mode.

Enzymatic synthesis is a significant approach used for obtaining pure cellulose via one-pot synthesis under aqueous conditions (Kobayashi et al. 2001; Kadokawa 2011). Cellulose oligomers can be synthesized using the reverse reaction of CDP from cellobiose as the acceptor and α-D-glucose 1-phosphate (αG1P) as the donor (Sheth and Alexander 1969; Arai et al. 1994; Samain et al. 1995; Reichenbecher et al. 1997; Krishnareddy et al. 2002). The precipitate previously synthesized using CDP with glucose as the acceptor was a plate-like cellulose II microcrystal with a thickness of 5 nm, corresponding to DP ≈ 9

(Hiraishi et al. 2009). The synthesis of reducing-end (RE) substituted cellulose oligomers was reported upon substitution of the acceptor with glucose derivatives: β-glucosyl azide, ^{13}C enriched D-glucose or deoxy-fluoro-D-glucose (Yataka et al. 2015; Kita et al. 2019; de Andrade et al. 2021). The RE unit was found to be located on both surfaces of the plate-like cellulose II microcrystals because of the antiparallel structure of cellulose II (Langan et al. 1999, 2001).

In this study, cellulose oligomers with azido groups introduced at the RE were enzymatically synthesized using CDP with β-glucosyl azide as the acceptor. It was found that the crystallites were sufficiently large for the magnetic orientation after recrystallization at a high temperature and did not aggregate in suspension owing to the repulsive dipolar interactions of the azido groups. Therefore, the static magnetic field orientation behavior of cellulose II was investigated using cellulose II microcrystals with the azido groups exposed on the surface.

Experimental

Enzymatic synthesis of cellulose oligomer

Recombinant CDP originating from the *Clostridium thermocellum* YM4 strain expressed in *Escherichia coli* was prepared and purified by the method described in a previous report (Krishnareddy et al. 2002). Sucrose phosphorylase (SP), which catalyzes the reaction of sucrose to α-D-glucose 1-phosphate (αG1P) and fructose in the presence of inorganic phosphate, was purchased from Oriental Yeast Co. (Tokyo, Japan). The cellulose oligomer was enzymatically synthesized using a combination of CDP and SP (Kita et al. 2019). CDP (0.05 U/mL) and SP (0.2 U/mL) were incubated in 40 mM phosphate buffer (pH 7.0) containing 50 mM glucose or 1-azido-1-deoxy-β-D-glucoside (β-glucosyl azide) as an acceptor and 400 mM sucrose at 40 °C for 72 h. After incubation, the cellulose oligomer obtained as an insoluble product was washed several times by centrifugation with distilled water. An aliquot of the sample was freeze-dried, while the rest of the sample was maintained in the suspension state until further use.

The freeze-dried samples were dissolved in 1% (w/v) lithium chloride/dimethylacetamide solution. The

size exclusion chromatogram (SEC) was recorded using a refractive index detector (RI-1530, JASCO, Japan) and a column (LF-804, SHODEX, Japan) at 50 °C with a flow rate of 0.5 mL/min. The DP was calibrated using pullulan standards (P-82, SHODEX, Japan). The average DP of both synthetic products obtained using glucose and β-glucosyl azide as acceptors was 10.

Recrystallization of cellulose oligomer

The freeze-dried cellulose oligomers (0.05–0.1%) were dispersed in distilled water, and the suspension was heated at 120–140 °C under a pressure of 0.2–0.4 MPa. After the cellulose oligomer was dissolved, the solution was slowly cooled to room temperature. Cellulose II microcrystals obtained by recrystallization were maintained in the suspension state until further use.

Electron microscopy and electron diffraction

Each of the suspensions containing approximately 0.05% of the samples before and after recrystallization was dropped on a thin carbon-coated copper grid hydrophilized by glow discharge, and excess water was removed using a filter paper followed by air drying. The specimen was shadowed with platinum at an angle of 30° using a BAF 400D apparatus (Balzers, Liechtenstein). The samples were observed using a transmission electron microscope (TEM) (JEM-1400, Jeol Co. Ltd., Tokyo, Japan) at 120 kV, and the electron micrographs were captured using a built-in CCD camera.

Electron diffraction was performed using a TEM (JEM-2000EXII, Jeol Co. Ltd., Tokyo, Japan) at 100 kV. Samples were irradiated with electron beams 100–200 nm in diameter, and the diffraction patterns were recorded on imaging plates (DITABIS Digital Biomedical Imaging System AG, Pforzheim, Germany). The camera length was calibrated using a diffraction ring of Au ($d_{1\ 1\ 1}$ = 0.2355 nm).

Alignment of cellulose microcrystals under the magnetic field

To facilitate handling of the cast film, the suspension of cellulose microcrystals having azido groups on the surface was mixed with 10% poly(vinyl alcohol) (PVA) solution (Kvien and Oksman 2007). The solution was prepared by dissolving PVA (Sigma-Aldrich Co., Mw 89,000–98,000, 99% hydrolyzed) in hot water and cooled to room temperature. The weight ratio of cellulose to PVA in the mixed suspension was 2:3. The suspension (200 μL) was poured into a plastic petri dish and dried overnight at 35 °C under a horizontal static magnetic field of 0 and 8 T generated using a cryogen-free superconducting magnet (Sumitomo Heavy Industries, Ltd., Tokyo, Japan) to obtain a cast film.

Synchrotron-radiated X-ray diffraction

Synchrotron X-ray diffraction (XRD) measurements of the cellulose microcrystal/PVA films were performed at the BL42B2 beamline located at the SPring-8 facility (Hyogo, Japan). The synchrotron-radiated X-rays (λ = 1.0 Å) were irradiated onto the film from three directions, as shown in Fig. 1. The diffraction patterns were recorded on a flat imaging plate (IP) (RAXIS V, Rigaku, Japan), and the sample-to-IP distance was calibrated using AgBeH powder ($d_{0\ 0\ 1}$ = 5.838 nm).

Results and discussion

Cellulose oligomers were synthesized from CDP using glucose and β-glucosyl azide as acceptors, and the average DP of each oligomer was 10. The low-dose bright-field images of the synthetic products captured
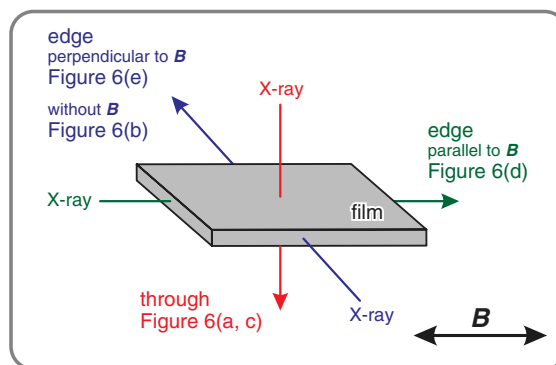

Fig. 1 Experimental layout used for X-ray diffraction of the films dried under static magnetic field of 8 T. Double-headed arrow indicates the direction of magnetic field. The film was irradiated with the X-ray beam from three directions as indicated by the arrows

before and after recrystallization via the diffraction contrast technique are shown in Fig. 2a–d. As shown, small and elongated rectangular microcrystals with rough edges overlapped and aggregated in the sample, just after synthesis and before recrystallization (Fig. 2a, c). The shape and size of the microcrystals were almost the same regardless of whether the acceptor was glucose or β-glucosyl azide. After recrystallization, small microcrystals grew to a few micrometers in length and hundreds to thousands of nanometers in width (Fig. 2b, d). The microcrystals with β-glucosyl azide were larger than those with glucose (Fig. 2d). The microcrystals were isolated, and their edges were sharp. The electron diffraction recorded from the encircled area of the isolated microcrystals indicated that the a^*b^* reciprocal lattice section of cellulose II exhibited a high degree of crystallinity (inset in Fig. 2d). From the relationship between microcrystal orientation and the electron diffraction diagram, the arrangement of the cellulose molecular chains in the microcrystals is shown in Fig. 3. The short side and long side of the microcrystals correspond to the (1 1 0) and (1 $\overline{1}$ 0) planes of cellulose II, respectively. A shadow-cast image of the
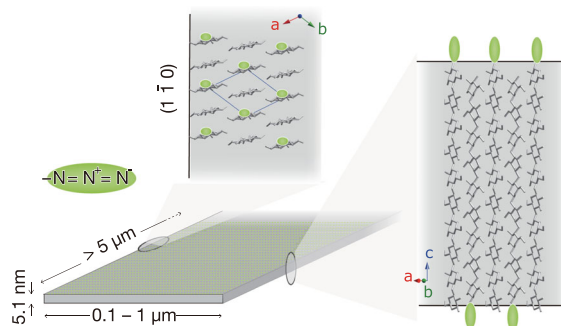
Fig. 3 Schematic of arrangement of cellulose molecules in cellulose II microcrystals. The azido groups are located on the surface of the cellulose II microcrystals

recrystallized microcrystals synthesized using β-glucosyl azide as the acceptor is shown in Fig. 2e. Each microcrystal was uniform in thickness, with an average value of 5.1 nm. This value corresponds to DP $\approx$ 10 as determined from the SEC measurement, which is ten times the length of the glucose unit, 0.5 nm. This result indicates that the chain axis of the cellulose is perpendicular to the base plane of the microcrystal; thus, azido groups are located on the surface of the microcrystals (Fig. 3).
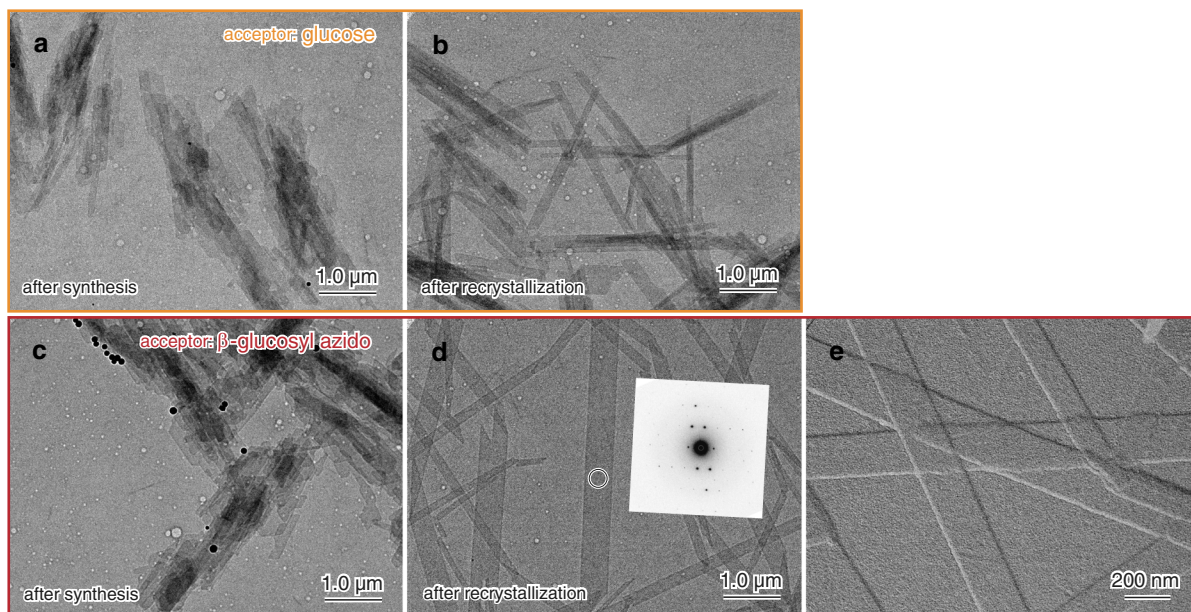

Fig. 2 Bright-field images of synthetic products using glucose **a**, **b** and β-glucosyl azide **c**, **d** as acceptor in the reaction of CDP and SP from sucrose before **a**, **c** and after **d**, **b** recrystallization obtained by the diffraction contrast technique. Inset in **d**: Electron microdiffraction diagram recorded from encircled area of the specimen showing the a^*b^* projection of cellulose II. **e** Shadow-cast image of the recrystallized sample shown in **d**. Platinum was evaporated onto the specimens with a shadowing angle of 30°

Flat ribbon-like microcrystals were formed by the recrystallization in water. The surface area of each face of the microcrystal followed the order of wide face > side face > > end face. The recrystallization in water accelerated crystal growth in the [1 1 0] direction because of the exposure of the hydrophobic moiety of the glucose ring to the (1 1 0) plane. Therefore, the [1 1 0] direction was the longest, and the area of the end face of the microcrystal was the smallest. The hydrophobicity of the side face could be slightly lower than that of the end face, resulting in lesser crystal growth in the [1 $\bar{1}$ 0] direction. Because the RE of the cellulose molecule is capped by the azido group, the molecular chains did not deposit in the c-axis direction. Even for the cellulose molecule without the azido group, the wide face is hydrophilic; thus, only the monomolecular layer is formed.

The suspension of the recrystallized samples at a concentration of 1 g/L was observed between the crossed polarizers (Fig. 4). Birefringence is commonly employed as an indicator of the dispersibility of microcrystals in a suspension (De Souza Lima and Borsali 2004). The suspension of microcrystals synthesized using β-glucosyl azide as the acceptor showed a stronger and brighter birefringence than that with glucose. In addition, the former showed better dispersibility than that of the latter. Moreover, the dispersibility of the suspension was maintained for several months. This result may be due to the repulsive dipolar interactions of the azido groups introduced on the surface of the cellulose II microcrystals.
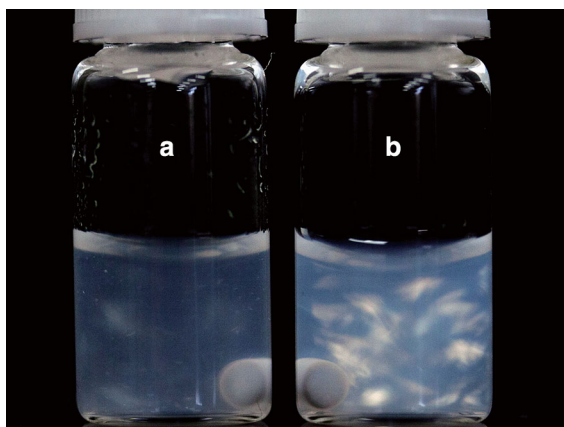

Fig. 4 Crossed polars image of 1 g/L microcrystal suspensions of cellulose II. Acceptors used for enzymatic synthesis were glucose **a** and β-glucosyl azide **b**

The suspension of recrystallized cellulose II microcrystals containing β-glucosyl azide was mixed with PVA solution and dried under a magnetic field of 8 T. Figure 5 shows the optical polarized micrographs of the cellulose II microcrystals/PVA film observed using a color plate. When the film was rotated by ± 45° with respect to the polarizing plate, it turned blue and yellow, which revealed that the cellulose II microcrystals were oriented in the film plane.
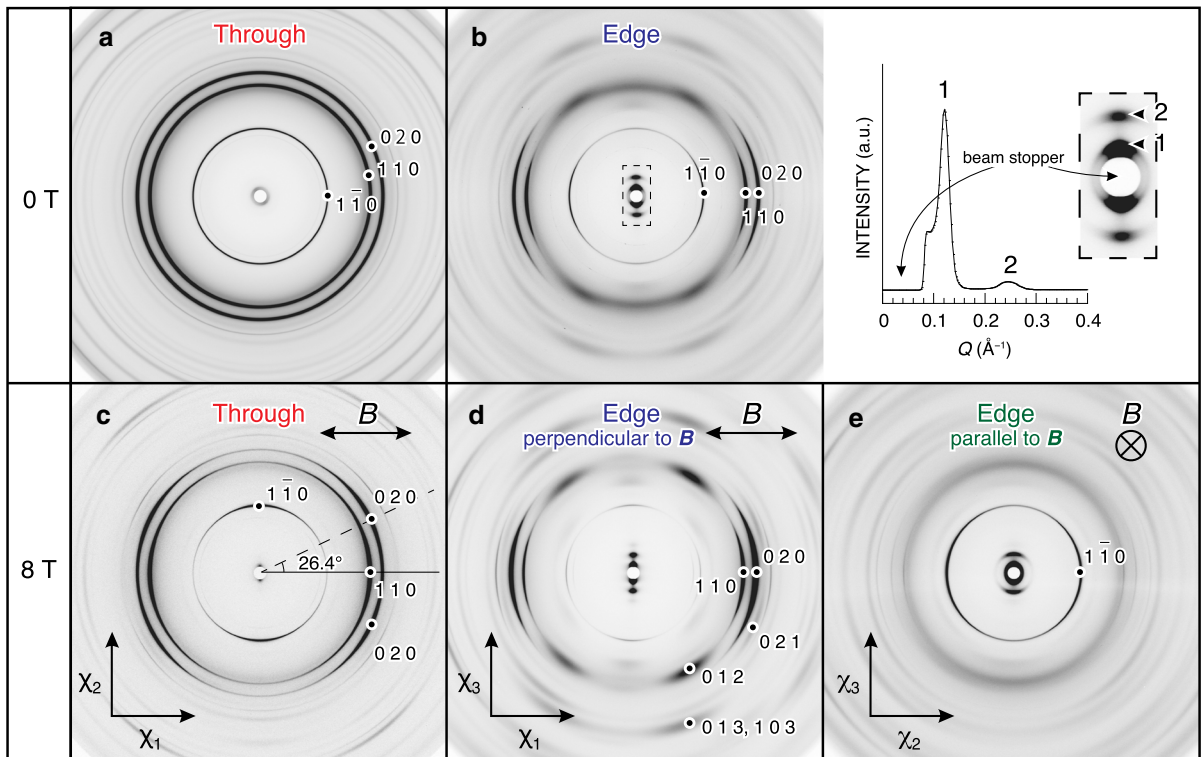
Synchrotron-radiated X-rays were irradiated onto the cellulose II microcrystals/PVA film dried with or without a magnetic field of 8 T (Fig. 1) to obtain the diffraction diagrams shown in Fig. 6. Figures 6a, b show the diffraction results obtained for the film dried without a magnetic field. In the through-view (Fig. 6a), the film exhibited three strong rings. These were assigned, from the low-angle side to the 1 $\bar{1}$ 0, 1 1 0, and 0 2 0 diffractions of cellulose II. On the other hand, these three diffractions exhibited strong arcs in the equator, in the edge-view (Fig. 6b). These observations indicate that the plate-like cellulose II microcrystals adopt a flat-on arrangement with respect to the film surface, that is, the molecular chains lie perpendicular to the film surface. Two strong diffractions observed on the meridian (Fig. 6b) at 5.2 nm and 2.6 nm can be attributed to the thickness of the cellulose II microcrystal, which correspond to the first- and second-order diffractions, respectively. The obtained value of 5.2 nm is similar to the thickness value determined for the shadow-cast images from TEM (5.1 nm) corresponding to cellulose chains with DP $\approx$ 10. From these results, we conclude that the cellulose molecular chain axis in the cellulose II microcrystal is aligned perpendicular to the film surface during drying, even without a magnetic field.

Figs, 6c, d, and e show the diffraction results obtained for the film dried under an 8 T magnetic field. Figure 6c shows the through-view diffraction profile obtained by impinging the X-rays perpendicular to the film surface (Fig. 1). The 1 1 0 diffraction appeared in the direction of the applied magnetic field, while the 1 $\bar{1}$ 0 and 0 2 0 diffractions appeared at 90° and 26.4°, respectively, from the direction of the magnetic field. By means of irradiating X-rays on the edge of the film perpendicular to the applied magnetic field direction (Fig. 1), a diffraction pattern similar to that in Fig. 6b was obtained, but the 1 $\bar{1}$ 0 diffraction almost disappeared in Fig. 6d. The intensity of 1 $\bar{1}$ 0
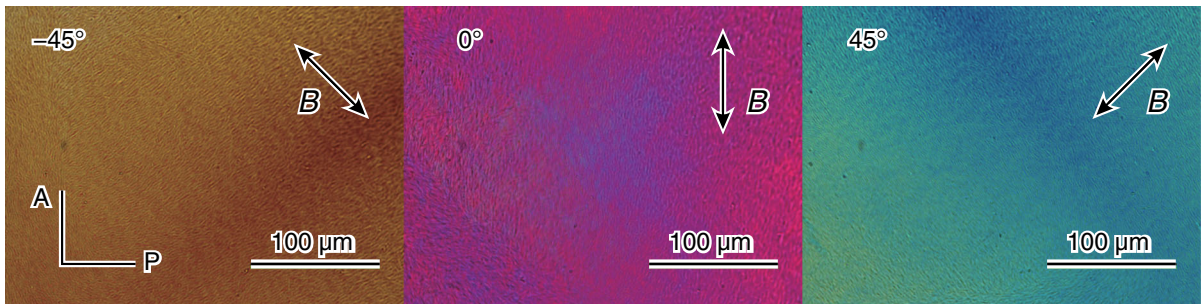
Fig. 5 Cellulose II crystals/PVA films dried under horizontal static magnetic field of 8 T were observed under polarized microscope with color plate. The double-headed arrow indicates direction of the magnetic field. The film was rotated by ± 45° with respect to the polarizer (P) and analyzer (A)

Fig. 6 Synchrotron-radiated X-ray diffraction diagrams of cellulose II microcrystals/PVA films dried under horizontal static magnetic field of 0 T **a**, **b** and 8 T **c**, **d**, **e**. The experimental layout of the X-ray diffraction measurements is shown in Fig. 1. The X-rays were irradiated perpendicular **a**, **c** (through-view) and parallel **b**, **d**, **e** to the film surface. The direction of applied static magnetic field during drying is indicated in the figure. The upper right figure is an enlarged view of the center part of the figure **b** surrounded by a dotted line and its diffraction intensity profile upward from the center, where Q is the scattering vector, $2\pi d^{-1}$ (Å^{-1})

diffraction was negligibly small (Fig. 6d). In contrast, by means of irradiating X-rays parallel to the magnetic field direction (Fig. 6e), the 1 1 0 and 0 2 0 diffractions disappeared, and 1 $\bar{1}$ 0 emerged. Therefore, the *c*-axis

and the [1 $\bar{1}$ 0] directions are aligned perpendicular to the magnetic field direction.

We conclude from the above XRD analysis that the [1 1 0] and [1 $\bar{1}$ 0] directions (approximately perpendicular to each other), are on the film surface, and the

[1 1 0] direction is aligned to the applied magnetic field. We find that this orientation is consistent with the polarized microscopy observations depicted in Fig. 5, which show that the film color turned blue upon rotation of the [1 1 0] direction by + 45°. This means that the relationship for the refractive indices is expressed by $n_{[110]} > n_{[1\bar{1}0]}$. According to the Lorentz–Lorenz equation, which relates the refractive index of a substance to its polarizability, the higher the linear density, the higher the refractive index. In the cellulose II crystals, the linear density is higher in the [1 1 0] direction than in the [1 $\bar{1}$ 0] direction because $d_{110} = 0.445$ nm and $= d_{1\bar{1}0} 0.726$ nm (Langan et al. 2001). Thus, the optical observations are consistent with the XRD results.

The three-dimensional orientation of microcrystals is usually achieved using time-dependent magnetic fields (Genoud et al. 1999; Kimura and Yoshino 2005). This orientation is also achieved by combining a static magnetic field and the confinement of one of the crystallographic axes, for example, using a flat-on arrangement of plate-like microcrystals, as in the present case. It is known that for the monoclinic crystal, one of the magnetic axes corresponds to the major axis (the c-axis in the present case), whereas two other magnetic axes are in the ab plane. We assume that the c-axis (chain axis) of the cellulose II microcrystal coincides with the χ_3 magnetic axis (the hard magnetization axis), similar to the case of the CNC. In the present study, the c-axis is oriented

uniaxially owing to the flat-on mechanism—that is, the χ_3 magnetic axis is confined perpendicular to the film surface. The χ_1 axis is aligned parallel to the magnetic field, resulting in the three-dimensional orientation of the magnetic χ_1, χ_2, and χ_3 axes. This does not necessarily mean that the crystallographic a, b, and c axes align three-dimensionally because the χ_1 and χ_2 axes do not coincide with the a and b axes. As a result, a twin orientation occurs. (Kimura et al. 2010).

Figure 7 shows the twin orientation of the reciprocal lattice (a) and real lattice (b) of the cellulose II crystal determined from the XRD diagrams (Fig. 6c–e). The twin orientation is ascribed to the monoclinic crystal form of cellulose II; the unique γ is not a right angle, but three-dimensional alignment is achieved by a static magnetic field. From the orientation of the cellulose II microcrystals, the direction of the magnetization axis of cellulose II could be determined. The angle between the 0 2 0 diffraction and the magnetic field direction calculated from the XRD diagram (Fig. 6c) was 26.4°; thus, the easy magnetization axis (χ_1) was the direction in which glucose rings were hydrophobically stacked similar to those in cellulose I (Sugiyama et al. 1992) but deviated by about 7° from the [1 1 0] direction. It is known that the hard magnetization axis (χ_3) of cellulose I is the direction of the molecular chain axis (Revol et al. 1994; Kimura et al. 2005). Since the molecular conformations of cellulose I and II are similar, the χ_3 axis of cellulose II would be the direction of the molecular chain axis. The 1 $\bar{1}$ 0 diffraction appeared at 90° from the magnetic
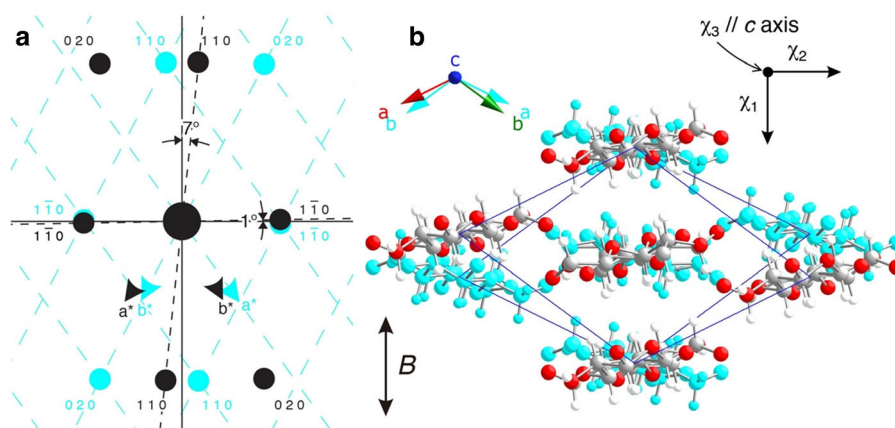
Fig. 7 Twin orientation of **a** reciprocal lattice and **b** real lattice f cellulose II crystals by the static magnetic field. A double-headed arrow indicates the direction of the magnetic field. The [1 1 0] and [1 $\bar{1}$ 0] directions are tilted by about 7° and 1° from χ_1

and χ_2 directions, respectively. The chain axis (c-axis) direction$\|\chi_3$ is perpendicular to the plane of the paper

field direction (Fig. 6c). Therefore, the intermediate magnetization axis (χ_2) is in the [1 $\bar{1}$ 0] direction, but it is tilted by approximately 1° as calculated from the relationship between the χ_1 axis and the [1 1 0] direction.

The following relationship exists between the half-width (H_w) in the X-ray azimuthal (β-I) plot and the magnetic field strength (B),

$$H_w(\text{rad}) = 2.35\sqrt{\frac{\mu_0 k_B T}{V|\chi_a|}}\frac{1}{B}$$

where μ_0 is the magnetic permeability of the vacuum, k_B is the Boltzmann constant, T is the absolute temperature, V is the volume of the microcrystal, and $|\chi_a|$ is the absolute value of anisotropy of the magnetic susceptibility ($\chi_a = \chi_1 - \chi_2$) (Kimura and Yoshino 2005; Kimura and Kimura 2018). The half widths calculated by the peak separation from the azimuthal plot of 1 $\bar{1}$ 0 and 1 1 0 in the XRD pattern (Fig. 6c) were 23.1° and 28.4°, respectively. The volume of the microcrystals was approximately $V = 200(\mu m) \times 4(\mu m) \times 5.1(\text{nm}) = 4.0 \times 10^{-21}(\text{m}^3)$. Upon substitution of these values into the above equation, the $|\chi_a|$ of cellulose II is 2.0–3.0 × 10^{-7}. This value is close to the theoretical (Pascal's principle) value $|\chi_a| = 3.6 \times 10^{-7}$ of cellulose I$_\beta$ (Frka-Petesic et al. 2015). The H_w value determined experimentally is usually larger than that determined using the above equation because the orientation loss due to solidification is added (Kimura et al. 2020). This leads to an underestimation of the $|\chi_a|$ value. However, this effect is minor when the crystal size is small, as in the present study. Thus, we can conclude that the $|\chi_a|$ of cellulose II is closer to that of cellulose I$_\beta$.

Declarations

Conflict of interest The authors declare their is no conflict of interest.

References

Arai M, Tanaka K, Kawaguchi T (1994) Purification and properties of cellobiose phosphorylase from Clostridium thermocellum. J Ferment Bioeng 77:239–242. https://doi.org/10.1016/0922-338X(94)90226-7

Bordel D, Putaux JL, Heux L (2006) Orientation of native cellulose in an electric field. Langmuir 22:4899–4901. https://doi.org/10.1021/la0600402

de Andrade P, Muñoz-García JC, Pergolizzi G et al (2021) Chemoenzymatic synthesis of fluorinated cellodextrins identifies a new allomorph for cellulose-like materials. Chem - A Eur J 27:1374–1382. https://doi.org/10.1002/chem.202003604

De Souza Lima MM, Borsali R (2004) Rodlike cellulose microcrystals: structure, properties, and applications. Macromol Rapid Commun 25:771–787. https://doi.org/10.1002/marc.200300268

Dong XM, Gray DG (1997) Induced circular dichroism of isotropic and magnetically-oriented chiral nematic suspensions of cellulose crystallites. Langmuir 13:3029–3034. https://doi.org/10.1021/la9610462

Frka-Petesic B, Sugiyama J, Kimura S et al (2015) Negative diamagnetic anisotropy and birefringence of cellulose nanocrystals. Macromolecules 48:8844–8857. https://doi.org/10.1021/acs.macromol.5b02201

Genoud J, Staines M, Mawdsley A et al (1999) Biaxially textured YBCO coated tape prepared using dynamic magnetic grain alignment. Supercond Sci Technol. 12:663–671. https://doi.org/10.1088/0953-2048/12/10/303

Habibi Y, Heim T, Douillard R (2008) AC electric field-assisted assembly and alignment of cellulose nanocrystals. J Polym Sci Part B Polym Phys 46:1430–1436. https://doi.org/10.1002/polb.21479

Hiraishi M, Igarashi K, Kimura S et al (2009) Synthesis of highly ordered cellulose II in vitro using cellodextrin phosphorylase. Carbohydr Res 344:2468–2473. https://doi.org/10.1016/j.carres.2009.10.002

Kadokawa J (2011) Precision polysaccharide synthesis catalyzed by enzymes. Chem Rev 111:4308–4345. https://doi.org/10.1021/cr100285v

Kimura F, Kimura T (2009) Three-dimensional orientation of cellulose crystals under dynamic elliptic magnetic field. J Phys Conf Ser. https://doi.org/10.1088/1742-6596/156/1/012002

Kimura F, Kimura T (2018) Magnetically textured powders-an alternative to single-crystal and powder X-ray diffraction methods. CrystEngComm 20:861–872. https://doi.org/10.1039/c7ce01305a

Kimura T, Yoshino M (2005) Three-dimensional crystal alignment using a time-dependent elliptic magnetic field. Langmuir 21:4805–4808. https://doi.org/10.1021/la050182g

Kimura F, Kimura T, Tamura M et al (2005) Magnetic alignment of the chiral nematic phase of a cellulose microfibril suspension. Langmuir 21:2034–2037. https://doi.org/10.1021/la0475728

Kimura F, Kimura T, Matsumoto K, Metoki N (2010) Single-crystal neutron diffraction study of pseudo single crystal prepared from microcrystalline powder. Cryst Growth Des 10:48–51. https://doi.org/10.1021/cg901321h

Kimura T, Kashiwagi H, Kimura F et al (2020) Orientation loss of microcrystals of DyBa2Cu3O: Yin a polymer composite during curing of the medium under an external magnetic field. CrystEngComm 22:5606–5612. https://doi.org/10.1039/d0ce00795a

Kita Y, Kusumi R, Kimura T et al (2019) Surface structural analysis of selectively 13C-labeled cellulose II by solid-state NMR spectroscopy. Cellulose 27:1899–1907. https://doi.org/10.1007/s10570-019-02896-x

Klemm D, Kramer F, Moritz S et al (2011) Nanocelluloses: a new family of nature-based materials. Angew Chemie - Int Ed 50:5438–5466. https://doi.org/10.1002/anie.201001273

Kobayashi S, Sakamoto J, Kimura S (2001) In vitro synthesis of cellulose and related polysaccharides. Prog Polym Sci 26:1525–1560. https://doi.org/10.1016/S0079-6700(01)00026-0

Krishnareddy M, Kim Y-K, Kitaoka M et al (2002) Cellodextrin phosphorylase from clostridium thermocellum YM4 strain expressed in escherichia coli. J Appl Glycosci 49:1–8. https://doi.org/10.5458/jag.49.1

Kvien I, Oksman K (2007) Orientation of cellulose nanowhiskers in polyvinyl alcohol. Appl Phys A Mater Sci Process 87:641–643. https://doi.org/10.1007/s00339-007-3882-3

Langan P, Nishiyama Y, Chanzy H (1999) A revised structure and hydrogen-bonding system in cellulose II from a neutron fiber diffraction analysis. J Am Chem Soc 121:9940–9946. https://doi.org/10.1021/ja9916254

Langan P, Nishiyama Y, Chanzy H (2001) X-ray structure of mercerized cellulose II at 1 Å resolution. Biomacromol 2:410–416. https://doi.org/10.1021/bm005612q

Marchessault RH, Morehead FF, Walter NM (1959) Liquid crystal systems from fibrillar polysaccharides. Nature 184:632–633

Nilakantan P (1938) Magnetic anisotropy of naturally occurring substances. Proc Indian Acad Sci - Sect A 7:38–49. https://doi.org/10.1109/tmag.1977.1059528

Nishiyama Y, Kuga S, Wada M, Okano T (1997) Cellulose microcrystal film of high uniaxial orientation. Macromolecules 30:6395–6397. https://doi.org/10.1021/ma970503y

Preston RD, Ripley GW (1954) Electron diffraction diagrams of cellulose microfibrils in Valonia. Nature 174:76–77. https://doi.org/10.1038/174076a

Pullawan T, Wilkinson AN, Eichhorn SJ (2012) Influence of magnetic field alignment of cellulose whiskers on the mechanics of all-cellulose nanocomposites. Biomacromol 13:2528–2536. https://doi.org/10.1021/bm300746r

Rånby BG (1949) Aqueous Colloidal Solutions of Cellulose Micelles. Acta Chem Scand 649–650. https://doi.org/10.3891/acta.chem.scand.03-0649

Rånby BG (1951) The colloidal properties of cellulose micelles. Discuss Faraday Soc 11:158–164. https://doi.org/10.1039/DF9511100158

Rånby BG, Ribi E (1950) Über den Feinbau der Zellulose. Protoplasma 6:12–14. https://doi.org/10.1007/BF02154044

Reichenbecher M, Lottspeich F, Bronnenmeier K (1997) Purification and properties of a celiobiose phosphorylase (CepA) and a cellodextrin phosphorylase (CepB) from the cellulolytic thermophile Clostridium stercorarium. Eur J Biochem 247:262–267. https://doi.org/10.1111/j.1432-1033.1997.00262.x

Revol JF, Godbout L, Dong XM et al (1994) Chiral nematic suspensions of cellulose crystallites; phase separation and magnetic field orientation. Liq Cryst 16:127–134. https://doi.org/10.1080/02678299408036525

Samain E, Lancelon-Pin C, Férigo F et al (1995) Phosphorolytic synthesis of cellodextrins. Carbohydr Res 271:217–226. https://doi.org/10.1016/0008-6215(95)00022-L

Sheth K, Alexander K (1969) Purification and glucosyltransferase properties : orthophosphate glucosyltransferase from Clostridium thermocellum. J Biol Chem 244:457–464

Song G, Kimura F, Kimura T, Piao G (2013) Orientational distribution of cellulose nanocrystals in a cellulose whisker as studied by diamagnetic anisotropy. Macromolecules 46:8957–8963. https://doi.org/10.1021/ma401788c

Sugiyama J, Chanzy H, Maret G (1992) Orientation of cellulose microcrystals by strong magnetic fields. Macromolecules 25:4232–4234. https://doi.org/10.1021/ma00042a032

Yataka Y, Sawada T, Serizawa T (2015) Enzymatic synthesis and post-functionalization of two-dimensional crystalline cellulose oligomers with surface-reactive groups. Chem Commun 51:12525–12528. https://doi.org/10.1039/C5CC04378F